

## An Improved Dilatometer for Polymers Based on Beta-Particle Absorption

S. MARTIN-LÖF and CH. SÖREMARK,\*

*Swedish Forest Products Research Laboratory and Rheological Laboratory at the Royal Institute of Technology, Stockholm, Sweden*

### Synopsis

The theoretical background and the operation of a new dilatometric technique based on the absorption of beta particles is described. The thermal expansion of the samples is determined by their change in weight per unit area with change in temperature. The experimental accuracy in a determination of a relative change in weight per unit area is, at a counting time of  $10^3$  sec, approximately  $4 \times 10^{-5}$ , which is close to the theoretical value. The applicability of the new device is illustrated by six runs on five different samples, among which hygroscopic and porous samples are represented. The temperature range covered is  $-60^\circ$  to  $+70^\circ\text{C}$ .

### INTRODUCTION

Radiometric methods for the determination and control of the weight per unit area of foil, fabric, paper, and a number of other materials are common industrial practice. Normally, such methods are based on the absorption of beta radiation. An attempt to utilize a method of this type for dilatometric purposes was made in 1962 by Zanetti and co-workers.<sup>1</sup>

The results of the dilatometric measurement were, however, not wholly compatible with common experience, although, for instance, the glass transition points could be indicated. Later, Klason and co-workers<sup>2</sup> attempted to build an improved device based on the same measuring principle. Their results were consistent with normal volume-temperature curves, even though the accuracy attainable and the reproducibility of the results were not sufficiently high for the purpose the device was intended for, i.e., for the study of comparatively weak secondary transitions in polymers.

The present paper describes a radiometric device basically similar to those described earlier<sup>1,2</sup> but with significant improvements. The high accuracy and reproducibility of the measurements are especially to be mentioned. This will be illustrated by a number of experimental examples, where even weak secondary transitions (for instance, in carbohydrates) can easily be resolved.

\* Present address: Swedish Forest Products Research Laboratory, Stockholm, Sweden.

The paper is divided into a theoretical section, dealing with the optimization of the conditions for attaining maximum sensitivity and accuracy, and an experimental section where the device is described and its function illustrated by actual dilatometric records. In an appendix, a statistical method for the evaluation of the dilatometric volume-temperature plots is presented. Special attention is paid to discontinuities (transitions) in such plots.

### THEORETICAL CONSIDERATIONS

In general, the absorption of beta particles may be represented<sup>3</sup> by the expression

$$T = \frac{N}{N_0} = \exp(-\mu_m \omega) \quad (1)$$

where  $T$ ,  $N$ , and  $\omega$  denote the transmission, the counts registered per unit time (intensity), and the weight per unit area of the absorber, respectively. The mass absorption coefficient  $\mu_m$  is related to the half-thickness as follows:  $\mu_m = \ln 2/\omega_{1/2}$ . An experimental plot of the intensity  $N$  versus the weight per unit area of cellulose samples is shown in Figure 1. For a given geometry, eq. (1) is valid only within a limited range of weights per unit area, because of the interaction between beta particles and the substance (scattering, excitation).

The value of the mass absorption coefficient is determined largely by the maximum energy ( $E_{\text{max}}$ ) of the emitted beta particles and by the atomic number of the absorbing substance, and to some extent by the geometry of the system. The coefficient increases when  $E_{\text{max}}$  decreases and when the atomic number increases.<sup>3</sup> If the absorber consists of more than one element, the resulting  $\mu_m$  can be calculated from the weight fraction  $x_i$  and the absorption coefficient  $\mu_{m,i}$  of each component according to the equation

$$\mu_m = \sum_{i=1}^n x_i \mu_{m,i} \quad (2)$$

For constant  $\mu_m$ , eq. (1) gives

$$-\frac{\delta N}{N} = \mu_m \delta \omega \quad (3)$$

In order to obtain the greatest change in the registered counts at a given  $\delta \omega$ , the value of  $\mu_m$  should, according to eq. (3), be high, corresponding to a low maximum energy of the beta particles. However, too low a value of  $E_{\text{max}}$  may cause difficulties in preparing thin durable samples. Among the other factors to be taken into consideration when selecting a radionuclide for the source are the specific and total activities, the contribution by gamma radiation, and the half-life.

For a given source, the theoretical optimal accuracy in the determination of a change in the weight per unit area according to eq. (3) may be calculated

as follows. If the Bremsstrahlung is considered almost constant (see Fig. 1), eq. (1) can be rewritten as

$$N = N_{\beta_0} \exp(-\mu_m \omega) + N_B = N_{\beta} + N_B \quad (4)$$

where  $N_{\beta_0}$  is the intensity of beta particles when  $\omega = 0$ , and  $N_B$  is the contribution by the Bremsstrahlung and the background. The differentiated form of eq. (4) may be written

$$-\frac{\delta\omega}{\omega} = \frac{\delta N}{\mu_m N_{\beta} \omega} \quad (5)$$

where  $\delta\omega/\omega$  is proportional to the coefficient of thermal expansion of the sample. Since the disintegrations are Poisson distributed, there is an error in the total number of counts, which is  $\sqrt{NS}$  (where  $S$  denotes the counting time). The standard error of  $\delta\omega/\omega$  may thus be written (neglecting high order terms) as follows:

$$\sigma \frac{\delta\omega}{\omega} = \frac{\sqrt{2N}}{\mu_m \omega N_{\beta} \sqrt{S}} \quad (6)$$

If, as a first approximation,  $N_{\beta}$  is put equal to  $N$ , the optimal weight per unit area is obtained by differentiating eq. (6) with respect to  $\omega$ . The derivative is zero when

$$\omega = \frac{2}{\mu_m} \quad (7)$$

This also corresponds to a minimum in the error incurred in determining the coefficient of thermal expansion.

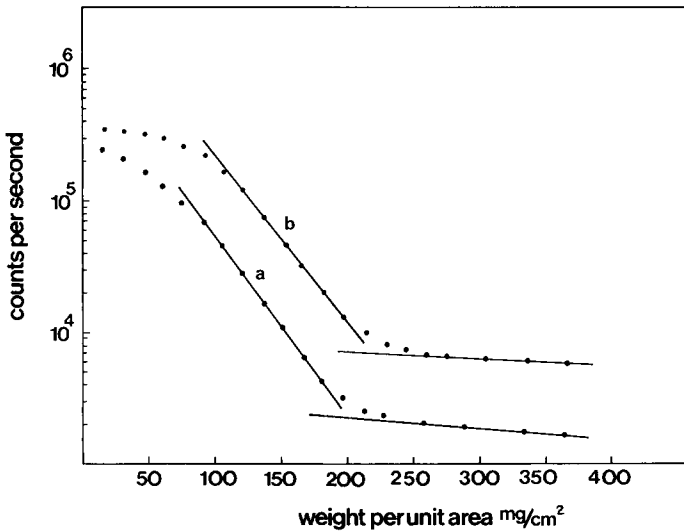


Fig. 1. Transmission of beta particles from  $^{204}\text{Tl}$  in cellulose with two source-to-detector distances: (a) 14 cm; (b) 7 cm.

For optimal accuracy, then, eq. (1) must be valid ( $\mu_m$ , maximum), the weight per unit area must be as close as possible to  $2/\mu_m$ , and the maximum number of counts must be registered. The counts are dependent not only on the counting time but also on the activity of the source, the source-to-detector distance, and the detector efficiency. The accuracy at two distances has been calculated from eq. (6) for a counting time of  $10^3$  sec. The values of  $N$  and  $N_\beta$  are taken from Figure 1. Figure 2 shows this accuracy as a function of the weight per unit area of cellulose, where the shortest source-to-detector distance is the practical minimum. It is seen that the highest accuracy,  $\sigma(\delta\omega/\omega)$ , is approximately  $3 \times 10^{-5}$ , corresponding to an error in the relative change in the total counts of approximately  $1.2 \times 10^{-4}$ .

## EXPERIMENTAL

### Apparatus

The experimental arrangement, with the detector and sample chamber, is shown in Figure 3. The source, selected as indicated above, was  $^{204}\text{Tl}$ , with an  $E_{\text{max}}$  value of 0.77 MeV, a half-life of 3.76 years, and an activity of approximately 6 mCi. It is of gold, with a circular active surface, 10 mm in diameter, covered by an ultrathin foil of gold (manufactured by Amersham Radiochemical Centre, Amersham, England). The sample, placed upon the the source, was inserted in the brass sample chamber, the design of which is shown in Figure 4. In order to eliminate any temperature gradient in the sample, the source and the sample were covered by a small foil cap. The absorption by this foil together with that by the foil separating the sample chamber from the overlying space was only about  $10^{-3}\%$ , and a negligible contribution to the observed change in transmission with temperature was

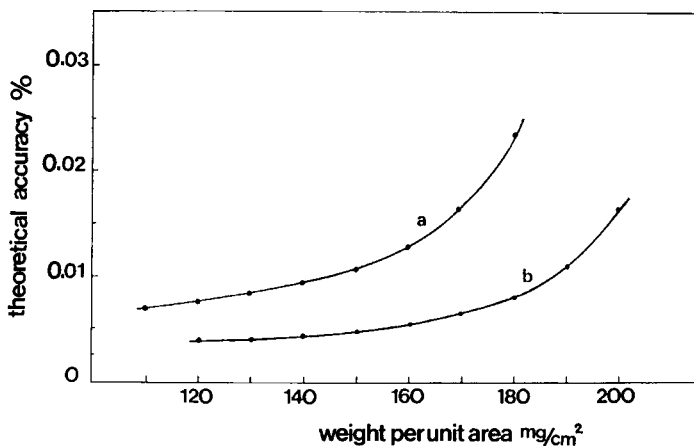


Fig. 2. Theoretical accuracy for a counting time of  $10^3$  sec in the determination of a relative change in weight per unit area at a level of significance of 67%. Source-to-detector distances: (a) 14 cm; (b) 7 cm.

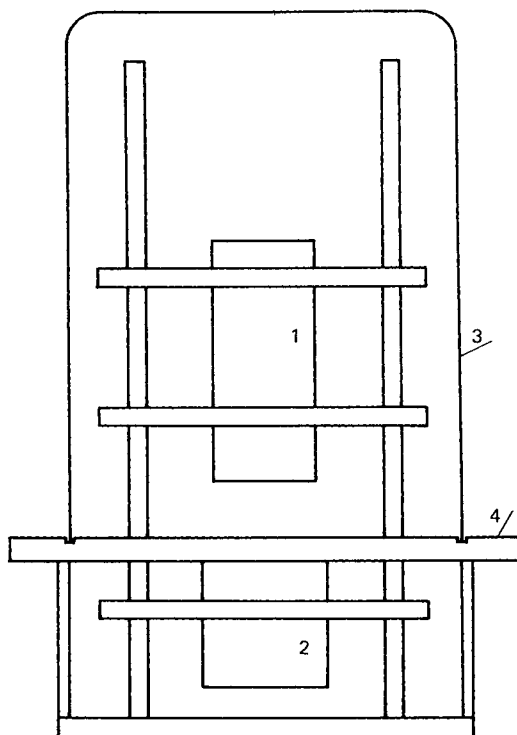


Fig. 3. The dilatometer: (1) detector; (2) sample chamber; (3) glass fan; (4) aluminum plate.

obtained. The connection between the dilatometer and the various auxiliary systems is shown schematically in Figure 5. Around the sample chamber, a circulation of ethanol or glycerin was maintained. The former was thermostated by means of a cryostat (Lauda 80 W), which keeps the temperature of the liquid within  $\pm 0.05^\circ\text{C}$ . This cryostat operates from  $-90^\circ$  to  $+60^\circ\text{C}$ , and above this level glycerin from a thermostat (Lauda NS 8/12) was used, which also maintains a steady temperature within  $\pm 0.05^\circ\text{C}$ .

The gas feed to the sample chamber was prethermostated (Fig. 4). The temperature of the sample chamber was measured with a platinum resistance thermometer connected with a linear bridge (Rosemount Engineering Co. Ltd., Model E 32000). This temperature was calibrated against that of the sample. The temperature in the space around the detector was determined in the same way and, with that of the sample chamber, was registered to an accuracy of  $\pm 0.03^\circ\text{C}$  on a six-channel recorder (Jaque, Type KSQ 306). The temperature of the gas surrounding the detector was kept constant at  $25^\circ\text{C}$  throughout the runs by means of constant cooling (water in copper tubes) and an adjustable heating (light bulbs). The gas was vigorously mixed by three fans. Close to the gap between the sample chamber and the

detector was a platinum resistance thermometer, which controlled a PID unit (Eurotherm, Model PID/SCR-10), to which the heating system was connected.

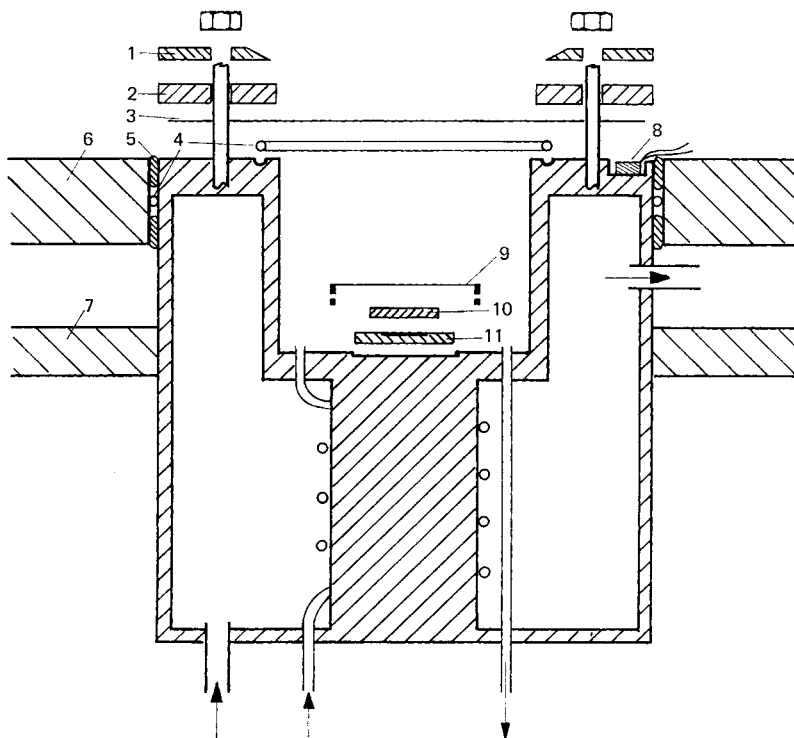


Fig. 4. Construction of sample chamber: (1) insulation ring of PVC; (2) brass ring; (3) sheet of Saran; (4) rubber ring; (5) sealing; (6) aluminum plate; (7) ring of bakelite for stabilization of the chamber; (8) platinum resistance thermometer; (9) cap of aluminum and Saran; (10) sample; (11) radioactive source.

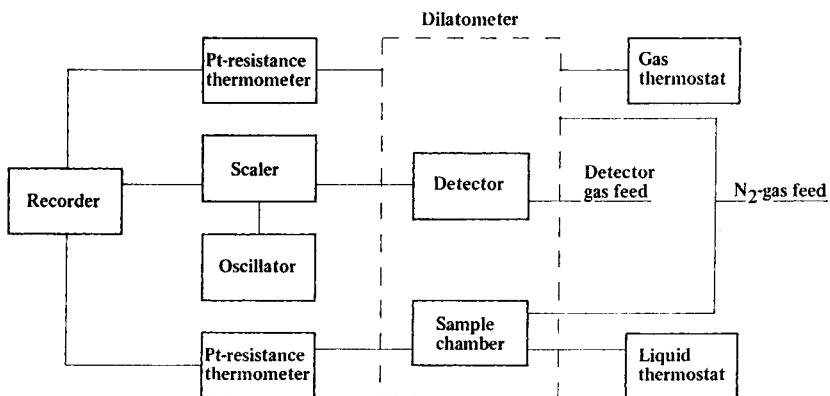


Fig. 5. The dilatometer and auxiliary systems.

A gas flow proportional counter (Picker, Model 64 1200) was used as a detector for the beta particles. A scaler (Spectroscaler III A), a translator, and a printer (all manufactured by Picker) were used for automatic registration of the beta particles. The Spectroscaler was modified by the addition of an external oscillator to provide a time base. In order to avoid condensation on the sample chamber and to ensure a constant composition of the gas, i.e., a constant absorption of the beta particles in the gas, a constant current of dried nitrogen was passed through the space around the detector. A stream of dry nitrogen was likewise passed through the sample space of the chamber. In order to replace the air rapidly with nitrogen, when the sample was changed, a high flow rate of the two currents was used at first. During the runs, the flows are kept constant at approximately 5 ml/min. The moisture content of the dried gas was less than 1 ppm (by volume). (It is, of course, possible to use other gases and other moisture contents in the sample chamber.)

### Experimental Errors

Besides the discussed statistical error, there are other errors that may affect the total accuracy of the dilatometer, such as those due to fluctuation in counting time, in temperature and pressure of the gas between the sample and the detector, and in temperature and homogeneity of sample.

In order to avoid errors in the counting time caused by fluctuation in the mains frequency ( $50 \pm 0.05$  Hz), a crystal oscillator, with an accuracy of  $10^{-6}$ , was used as a time base.

The variation in the temperature of the gas between the sample and the detector was kept within  $\pm 0.1^\circ\text{C}$ . According to eq. (3), this corresponds to an error in the counts during  $10^3$  sec of  $4 \times 10^{-5}$ , which is negligible. Since the gases had free outlets, there was no variation in the pressure apart from that in atmospheric pressure, which was registered and, if necessary, compensated for. The temperature of the sample was kept constant within  $\pm 0.05^\circ\text{C}$ . According to eq. (3) and assuming a coefficient of thermal expansion  $\lambda$  of  $10^{-4} \text{ }^\circ\text{C}^{-1}$ , this also implies a negligible error.

It should also be noticed that irregularities in the weight per unit area of the sample result in a wrong value of  $\lambda$ . This can be explained as follows. Let the weight per unit area vary with respect to the mean  $\omega_0$  as follows:

$$\omega = \omega_0 + \delta\omega \quad (8)$$

and let

$$\int_A (\omega + \delta\omega) dA = \omega_0 \quad (9)$$

Equation (1) can be written

$$N = N_0 \int_A \left[ \exp(-\mu_m \omega_0) \left( 1 - \mu_m \delta\omega + \frac{\mu_m^2 (\delta\omega)^2}{2} \dots \right) \right] dA \quad (10)$$

Since  $\int_A \mu_m \delta \omega dA = 0$ , the error will depend only on the second-order factor if higher orders are neglected. If, to a first approximation, a fraction  $\alpha$  and a fraction  $1 - \alpha$  have the weight per unit area  $\omega_1$  and  $\omega_2$ , respectively, we can write

$$\frac{\mu_m^2 (\delta \omega)^2}{2} dA = \frac{\mu_m^2 A}{2} [\alpha (\omega_1 - \omega_2)^2 + (1 - \alpha) (\omega_2 - \omega_1)^2]. \quad (11)$$

This means that the error  $\sigma(\delta N/N)$  depends on by how much eq. (11) deviates from zero. In the present case, the unevenness of the samples was checked by  $\beta$ -radiograms and naked-eye examination by transmitted light and found to be negligible.

### Evaluation of the Coefficient of Thermal Expansion

A change in the temperature of the sample will result in a change in the weight per unit area of the sample,  $\Delta \omega_s$ , and of the gas in the sample chamber,  $\Delta \omega_g$ . These two changes in weight per unit area will cause a change in the transmission of the beta particles in accordance with eq. (1). If  $N^0$  and  $N$  represent the intensities at the temperatures  $t^0$  and  $t$ , respectively, eq. (1) may be rewritten as follows:

$$\ln \frac{N^0}{N} = -\mu_{m,s} \Delta \omega_s - \mu_{m,g} \Delta \omega_g = -\mu_{m,s} (\Delta \omega_s + c_1 \Delta \omega_g) \quad (12)$$

It should here be pointed out that the change with temperature of the active area of the source behind the sample only affects the registered counts by its geometric change in relation to the detector. This change has been shown to be negligible in comparison with the above mentioned sources of changes in the intensity of the registered beta particles.

The plots in the present paper show this apparent change in weight per unit area with respect to the weight per unit area of the samples at  $t^0$  versus the temperature, according to the expression

$$\frac{\Delta \omega_s + c_1 \Delta \omega_g}{\omega_s^0} = \frac{\ln \frac{N^0}{N}}{\mu_{m,s} \omega_s^0} \quad (13)$$

Here, the exponent zero refers to conditions at 25°C.

The value of the coefficient of thermal expansion,  $\lambda$ , of the sample can be obtained from the curves since, to a close approximation,

$$\Delta \omega_s = \omega_s (\lambda_y + \lambda_z) \Delta t. \quad (14)$$

The coordinates  $y$  and  $z$  are perpendicular to the direction of the source detector. For homogeneous and isotropic substances,  $\lambda_y$  and  $\lambda_z$  are equal. The thermal expansion of the gas in the sample chamber can be represented by the expression

$$\Delta \omega_g = c_2 t \quad (15)$$



which, together with eq. (14), gives the slope of the curve

$$\frac{\Delta\omega_s + c_1\Delta\omega_g}{\omega_s^0\Delta t} = 2\lambda + \frac{c_1c_2}{\omega_s^0} \quad (16)$$

The constants  $c_1$  and  $c_2$  can easily be determined from a plot for a sample with a known  $\lambda$ , or they can be calculated from theory.

### Procedures and Materials

The measurements were carried out both by increasing and by decreasing the temperature of the sample through the relevant range. The temperature was usually changed in steps of 2.5°C every 20 min. As the counting time was 600 sec, the temperature was first equilibrated for 10 min.

The materials studied were polystyrene (PS), poly(methyl methacrylate) (PMMA), poly(tetrafluoroethylene) (Teflon), and aluminum, the specimens being machined to suitable dimensions. Cellulose and glucose monohydrate were pressed into discs in a KBr die (Perkin & Elmer). Relevant data concerning these materials are given in Table I. The weight per unit area of all the specimens was approximately 140 mg/cm<sup>2</sup>. During the measurements, all the samples were kept in nitrogen gas dried with phosphorus pentoxide.

TABLE I  
Some Characteristics of the Samples

<i>Poly(tetrafluoroethylene)</i> (du Pont)	
density, g/cm <sup>3</sup>	2.19
crystallinity, %	62 ± 5
<i>Poly(methyl methacrylate)</i> (Röhm & Haas)	
density, g/cm <sup>3</sup>	1.18
molecular weight	6 × 10 <sup>5</sup>
<i>Polystyrene, atactic</i> (Dow)	
density, g/cm <sup>3</sup>	1.04
molecular weight	8.5 × 10 <sup>5</sup>
<i>Aluminum</i> (Svenska Metallverken)	
density, g/cm <sup>3</sup>	2.70
purity, %	99.5
<i>Cellulose II</i>	
Prepared by conventional mercerization from ramie cellulose. <sup>9</sup>	
<i>Glucose monohydrate</i>	
Prepared by recrystallization from water at 5°C.	

In the plots, a value of  $\mu_m$  (29.0 cm<sup>2</sup>/g) from Figure 1, which represents the composition C<sub>6</sub>H<sub>10</sub>O<sub>5</sub>, was used. According to eq. (2), this value is almost constant for the carbohydrates, since the ratio C:H:O for these is nearly the same.

## RESULTS AND DISCUSSION

The linearity of the dilatometer was checked by measuring a calibrated sample of aluminum having a thermal expansion of

$$l_t = l_0[1 + (22.17t + 0.012t^2)10^{-6}].$$

The range of temperature studied was  $-65^\circ$  to  $+90^\circ\text{C}$ . From the slope of this plot and the known  $\lambda$ , a value of  $5.62 \times 10^{-3} \text{ }^\circ\text{C}^{-1}$  has been obtained for the product of the constants  $c_1$  and  $c_2$  in eq. (16). This is consistent with the theoretical value. Thus, the change in transmission with changing temperature arises only from the sample and the gas in the sample chamber.

Three polymeric materials, Teflon, PMMA, and PS, were examined in order to ascertain the possibilities of studying thermal transitions.

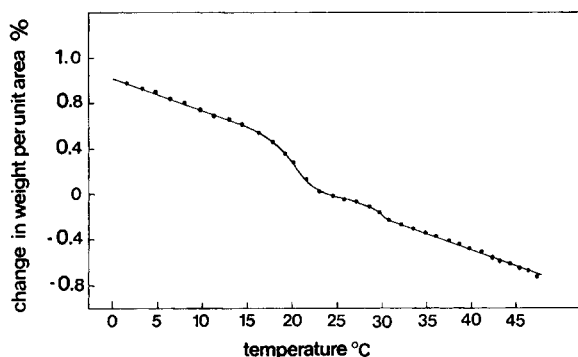


Fig. 6. Change in weight per unit area, relative to the value at  $25^\circ\text{C}$ , vs. temperature for poly(tetrafluoroethylene).

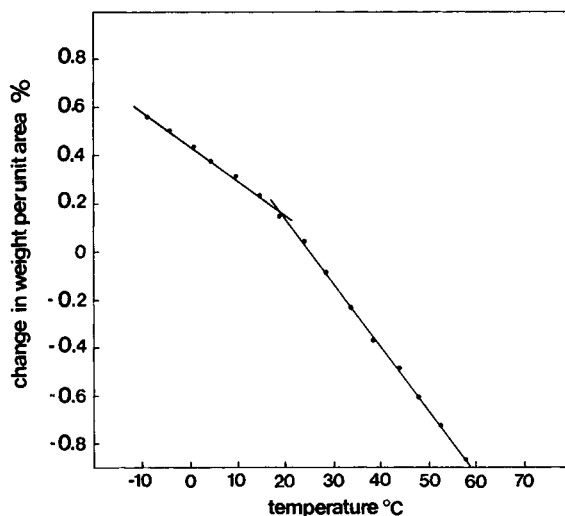


Fig. 7. Change in weight per unit area vs. temperature for poly(methyl methacrylate) during increase in temperature.

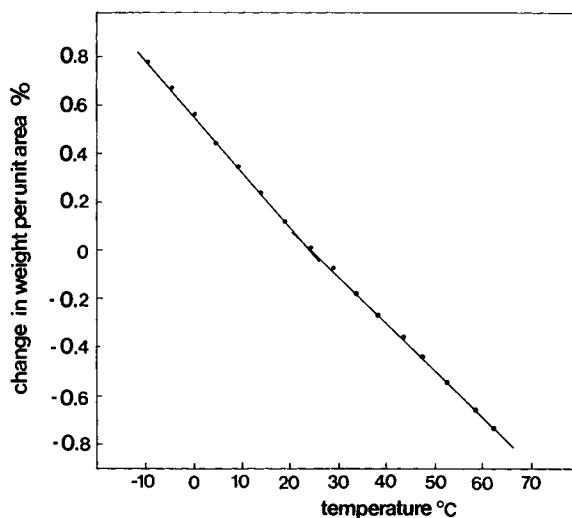


Fig. 8. Change in weight per unit area vs. temperature for poly(methyl methacrylate) during decrease in temperature.

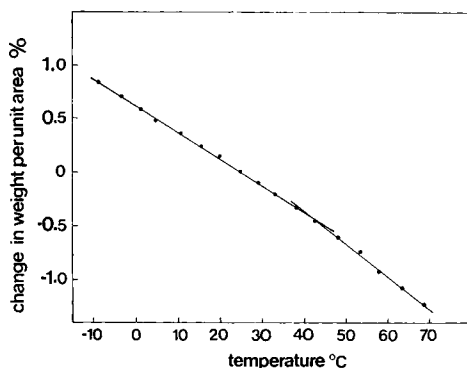


Fig. 9. Change in weight per unit area vs. temperature for polystyrene.

Teflon has two closely spaced first-order transitions, approximately  $300^{\circ}\text{C}$  below the melting point at  $20^{\circ}$  and  $30^{\circ}\text{C}$ .<sup>4,5</sup> As seen from Figure 6, which shows the thermal expansion between  $0$  and  $50^{\circ}\text{C}$ , these two transitions are clearly indicated. The temperature here was steadily raised at a rate of  $2.5^{\circ}\text{C}/\text{min}$ .

Several investigators using dilatometric and other techniques with a relatively long time scale have reported a secondary transition in PMMA in the interval from  $10^{\circ}$  to  $61^{\circ}\text{C}$ .<sup>6</sup> Figure 7 shows the thermal expansion when the temperature was increased from  $-15^{\circ}$  to  $65^{\circ}\text{C}$  in steps of  $2.5^{\circ}$  every 20 min. Figure 8 shows the effect of the corresponding decrease in temperature. The slope changes at approximately  $22^{\circ}\text{C}$ . When the temperature of the sample was decreased, a higher thermal expansion was observed below  $22^{\circ}\text{C}$ . This may be ascribed to an increase in the creep rate when passing through the transition region; confirmation of this is perhaps found in the

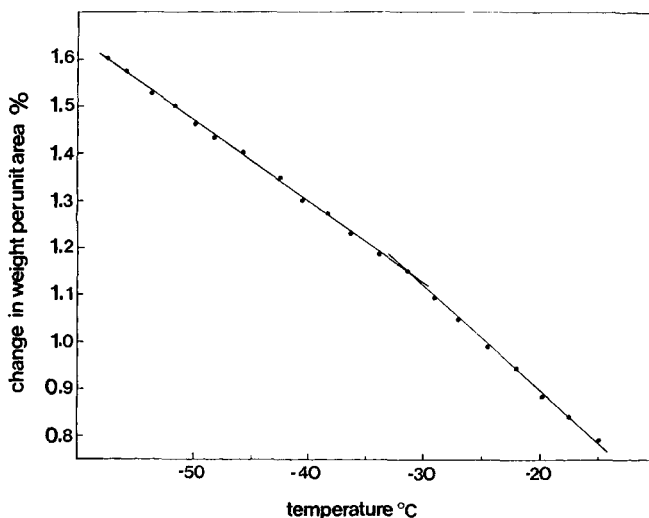


Fig. 10. Change in weight per unit area vs. temperature for cellulose II.

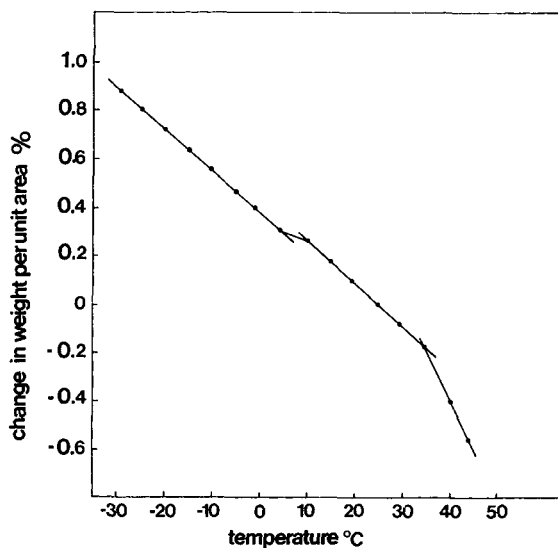


Fig. 11. Change in weight per unit area vs. temperature for  $\alpha$ -D-glucose monohydrate

fact that this change in slope at the transition point was found to depend on the heating rate.

The thermal expansion of PS in the interval from  $-15^{\circ}\text{C}$  to  $70^{\circ}\text{C}$  is shown in Figure 9. A secondary transition is indicated at approximately  $42^{\circ}\text{C}$ . This bears out the findings of other investigators, who have reported a secondary transition in the range  $40^{\circ}$  to  $60^{\circ}\text{C}$ .<sup>7,8</sup>

The relative change in weight per unit area with temperature was also studied on two carbohydrates, namely cellulose II and glucose monohydrate. The cellulose II was prepared from ramie cellulose by a conventional mer-

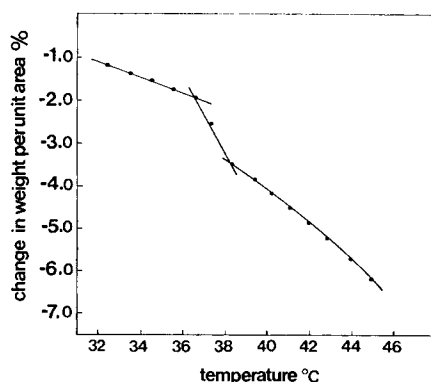


Fig. 12. Change in weight per unit area vs. temperature for  $\alpha$ -D-glucose monohydrate.

cerization technique,<sup>9</sup> and glucose monohydrate by recrystallization from water. As seen in Figure 10, there was a discontinuity in the thermal expansion of cellulose II at approximately  $-32^{\circ}\text{C}$ . This transition was first reported in cellulosic materials (Viscose rayon, Bemberg, and cotton slivers) by Ishida and co-workers,<sup>10</sup> who used a dielectric technique and later a torsion pendulum in cellulose I and II.<sup>11</sup>

On the other carbohydrates, glucose monohydrate, two runs are demonstrated. There were two transitions at approximately  $15^{\circ}$  and  $37^{\circ}\text{C}$  (Fig. 11). Here, a change of  $5^{\circ}\text{C}$  every 30 min was made. In Figure 12, where a change of  $1^{\circ}\text{C}$  was made every 20 min, a greater change in weight per unit area with temperature can be seen above the transition at  $37^{\circ}\text{C}$ , indicating a loss of mass through diffusion. A possible explanation of the transition at  $15^{\circ}\text{C}$  has been offered by Martin-Löf and Söremark.<sup>12</sup> The same authors have also verified that the transition at  $37^{\circ}\text{C}$ , first observed by using this dilatometer, is of the first order and associated with the loss of water of crystallization.<sup>12</sup>

All the plots presented were evaluated as shown in the Appendix. With the testing procedures described, the changes in slope at the transition points are significant at the 95% level. These tests are based on an experimentally determined standard deviation for each point. This error was calculated from 40 registrations of the total number of counts of  $10^3$  sec each, at a constant temperature. This procedure was repeated for some of the substances and at five temperature levels within the studied range. The highest indicated standard deviation,  $\sigma$ , of the relative change in the total number of counts during  $10^3$  sec was  $1.6 \times 10^{-4}$ . This corresponds to an error in the relative change in weight per unit area of  $4 \times 10^{-5}$ . As can be seen from Figure 2, this value is only slightly greater than the theoretical value; thus, all the errors that may affect the accuracy of the dilatometer were adequately controlled.

### CONCLUDING REMARKS

In most dilatometers, the change in size or volume with temperature is registered mechanically or optically. Unlike other types, the dilatometer

described in this paper can be characterized by the fact that there is no mechanical measurement of the specimen and that it registers the change in weight per unit area as a function of temperature. These two factors, combined with the high accuracy and the small size of the specimens, offer several unique properties. Some of these advantages are illustrated in the above applications.

### Appendix

With a reasonable degree of approximation we may consider the following statistical model: For a sequence of values of the temperature  $t$ , we make observations on the relative change in weight per unit area

$$y(t) = \frac{\Delta\omega}{\omega^0}$$

For each value of  $t$ ,  $y(t)$  is a normally distributed random variable. The mean value of  $y(t)$  is a linear or piecewise linear function of  $t$  with unknown coefficients and a small number of pieces. The standard deviation is a known constant independent of  $t$ .

The explanation of the reasons for the assumptions are as follows: (1) The higher order terms in the expansivity of the sample can, in these limited temperature ranges, be neglected. (2) The total change in the counting rate during a measurement is so small that the standard deviation of its determinations can, to a good approximation, be considered constant.

To control our model, we divide the temperature interval into subintervals, such that, we believe, the mean value function will be linear within each subinterval. After that, we use standard linear regression methods to test the linearity within each subinterval and to test for significant differences between the mean value functions in adjoining subintervals. The standard linear regression theory also yields estimators of, and confidence intervals for, the mean value function and its coefficients. For a detailed description of linear regression methods, we refer to Hald.<sup>13</sup>

The authors wish to express their gratitude to Professor J. Kubát for his interest and support. Thanks are also due to Miss Iréne Holmquist for her skillful experimental assistance. Financial support from Carl Trygger's Foundation for Scientific Research is gratefully acknowledged.

### References

1. R. Zanetti, P. Manaresi, and L. Baldi, *Chim. Ind. (Milan)*, **44**, 1114 (1962).
2. C. Klason, J. Kubát, and A. de Ruvo, *Rheol. Acta*, **6**, 390 (1967).
3. K. Siegbahn, *Alpha-, Beta-, and Gamma-Ray Spectroscopy*, Vol. 1, North-Holland Publishing Company, Amsterdam, 1966.
4. F. A. Quinn, Jr., D. E. Roberts, and R. N. Work, *J. Appl. Phys.*, **22**, 1085 (1951).
5. T. Yasuda and Y. Araki, *J. Appl. Polym. Sci.*, **5**, 331 (1961).
6. H. F. Atkinson and A. A. Grant, *Nature*, **211**, 627 (1966).
7. T. Holt and D. Edwards, *J. Appl. Chem.*, **15**, 223 (1965).
8. Y. Wada, H. Hirose, and T. Asano, *J. Phys. Soc. Japan*, **14**, 1064 (1959).
9. J. Kubát, S. Martin-Löf, and Ch. Söremark, *Svensk Papperstidn.*, **72**, 731 (1969).
10. Y. Ishida, M. Yōshino, and M. Takayanagi, *J. Appl. Polym. Sci.*, **1**, 227 (1959).
11. J. Kubát and C. Pattryanie, *Nature*, **215**, 390 (1967).
12. S. Martin-Löf and Ch. Söremark, *Svensk Papperstidn.*, **72**, 193 (1969).
13. A. Hald, *Statistical Theory with Engineering Applications*, Wiley, New York, 1952.

Received August 5, 1970